Results in Physics 60 (2024) 107653

Contents lists available at ScienceDirect

Results in Physics

journal homepage: www.elsevier.com/locate/rinp

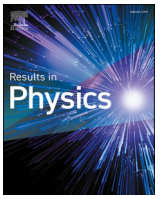

Temperature-dependent optical bandgap of TiO_2 under the Anatase and Rutile phases

A.R. Zanatta

Instituto de Física de São Carlos, Universidade de São Paulo, São Carlos, SP 13560-590, Brazil

ARTICLE INFO

Keywords:
Titanium dioxide TiO_2
Optical bandgap
Optical spectroscopy
Raman scattering
Solid state physics

ABSTRACT

A crucial step in developing new and/or more efficient devices relies on the detailed knowledge of the properties of their main (elemental or combined) parts. The same applies to titanium dioxide TiO_2 that forms the basis of today numerous applications whose performances are determined by the presence or relative amount of the Anatase (A-) and Rutile (R-) most common phases of TiO_2. Whereas the basic structural characteristics of these two polymorphs are very well-established, some of their optical aspects still deserve attention. With these ideas in mind this work presents a comprehensive investigation of the optical bandgap E_{gap} of TiO_2 under the Anatase and Rutile phases. The study considered pure A-TiO_2 and R-TiO_2 samples in the form of powder, and optical reflectance and Raman spectroscopy in the 83–823 K temperature range. In addition to reliable E_{gap} values the study explores their temperature-dependent $E_{gap}(T)$ behavior that is expected to assist future advancements in the field of TiO_2-based materials and devices (thin films, interfaces, low-dimensional systems, and photocatalytic and solar cells, for example).

Introduction

Titanium dioxide TiO_2 is a chemically-inert, relatively low-cost semiconductor material that has been inspiring research in the academic-technological areas for years [1]. In spite of its modest atom composition TiO_2 can exhibit distinctive atomic arrangements and, therefore, it is able to present completely different properties. When adopting the tetragonal crystal structure, for example, TiO_2 can exist under the Anatase A- (space group $I4_1/amd$, a = 3.7845 Å and c = 9.5143 Å) or Rutile R- (space group $P4_2/mnm$, a = 4.5937 Å and c = 2.9587 Å) phases [2]. Regarding the electronic properties there is certain consensus that the optical absorption edge of TiO_2 stays around 400 nm and that, whereas the bandgap of A-TiO_2 is indirect, most of the optical processes taking place in R-TiO_2 are of direct nature [3,4]. Moreover, it is known that the precise optical bandgap E_{gap} values are subject to sample details (morphology and purity, for example) as well as to the method-conditions of measurement. In fact, this is a matter of concern since small variations in the structure and composition of TiO_2 can lead to significant variations of E_{gap} [5–8], and because A-TiO_2 can be irreversibly transformed into R-TiO_2 above approx. 850 K - depending on several experimental conditions [9].

In addition to all of these characteristics, A-TiO_2 and R-TiO_2 represent the two most important polymorphs of TiO_2 and are at the origin of many successful achievements involving: photo- or solar-driven processes [10–13], environment sensors [14], energy storage [15], control-manipulation of biomolecules [16], and cosmetics, paints and coatings [17], just to mention a few of them. Actually, it is the combination of the structural and optical properties of the A-TiO_2 and R-TiO_2 phases that decides the application target and, specially, the performance of future TiO_2-based devices. A classical example of such influence refers to TiO_2-containing dye-sensitized solar cells where the presence of R-TiO_2 can act either improving the short-circuit current and number of photo-generated electrons [18,19], or partially compensating variations in the photo-electrode areas [20]. As a result, it seems clear that the development of new and/or improved TiO_2-based applications is conditioned to the precise identification-quantification [21,22] and detailed knowledge of the properties of the A-TiO_2 and R-TiO_2 polymorphs.

Specifically related to the temperature-dependent optical bandgap E_{gap} behavior of the Anatase and Rutile phases of TiO_2 the literature is still incomplete and very scarce. Apparently, there are three reports on the subject that, despite presenting some theoretical work, performed experiments basically with A-TiO_2 [23,24] or with (very thin) films [23,25] - in all cases, only above room-temperature.

Motivated by the basic-applied interest in TiO_2, as well as by the need of supplementary information, this work presents a comprehensive

E-mail address: zanatta@ifsc.usp.br.

https://doi.org/10.1016/j.rinp.2024.107653
Received 4 January 2024; Received in revised form 14 March 2024; Accepted 4 April 2024
Available online 5 April 2024

study of the temperature-dependent optical bandgap $E_{gap}(T)$ of the Anatase and Rutile polymorphs of TiO_2. In addition to the $E_{gap}(T)$ investigation (which also includes its analysis with some theoretical models) the work also presents the main structural-compositional data of the A-TiO_2 and R-TiO_2 samples.

Experimental details

The studied A-TiO_2 and R-TiO_2 correspond to commercial (Sigma-Aldrich 99.99 % pure) samples in the form of powders. The chemical (stoichiometric) composition of the samples was confirmed by energy dispersive x-ray (EDX) measurements, and the analyses of scanning electron microscopy images indicate that the samples present average grain sizes, typically, in the range of hundreds of nm (see SuppMater_Fig. S1).

Optical reflectance measurements were carried out in a system comprising a portable spectrometer (*Ocean Optics* HR4000), a deuterium-halogen UV–VIS-NIR light source (*Mikropack* DH-2000-BAL), and a bifurcated optical fiber (*Ocean Optics* BIF600-UV–VIS). The sample measured areas and the spectral resolution stayed around 3 mm^2 (2 mm spot diameter) and below 10 nm, respectively, and all spectra were corrected by the optical response of the system to ensure 100 % light reflection from a diffuse reflectance standard.

The structure of the A-TiO_2 and R-TiO_2 powders were investigated by Raman scattering spectroscopy (*Renishaw* RM2000) [22]. The measurements considered ~ 80 μm^2 sample surface areas and they were performed with low power (30 μW) HeNe 632.8 nm laser radiation.

The optical reflectance and Raman scattering spectra were acquired in the 83–823 K range (in steps of either 25 or 50 K) after leaving the samples at the desired temperature for 5 min. In this case a computer-controlled, nitrogen gas-purged T-stage (*Linkam* THMS600) was employed. Before each measurement the powders were assembled in a copper-made sample holder and gently pressed in order to obtain a compact and smooth sample surface. Even though the temperature-dependent measurements considered a rather small sample amount (150 mm^3) and a mild temperature rate (10 K/min), additional spectra were taken at 83, 173, 273, 523, and 773 K after 30 min. As will be shown, since the use of different dwelling times originated no appreciable changes in both reflectance and Raman spectra, it is reasonable to state that all measurements were obtained with the samples under thermal equilibrium conditions.

Experimental results

The optical diffuse reflectance spectra of the A-TiO_2 and R-TiO_2 samples, at some selected temperatures, are shown in Fig. 1. In the 225–550 nm range, where the optical absorption edges of TiO_2 are expected to occur [4], it is evident the evolution of the spectra as the temperature of measurement increases. These changes originate because of modifications in the (temperature-dependent and phonon-dependent) optical transitions that, ultimately, will determine the bandgap E_{gap} of the samples. (The complete set of diffuse reflectance spectra can be seen in SuppMater_Fig. S2.).

The Raman spectra of the very same samples are shown in Fig. 2 that, additionally, indicate the main phonon modes relating the A-TiO_2 [at approximately 144 cm^{-1} (E_g), 196 cm^{-1} (E_g), 395 cm^{-1} (B_{1g}), 518 cm^{-1} ($A_{1g} + B_{1g}$) and 639 cm^{-1} (E_g)] and R-TiO_2 phases [at 143 cm^{-1} (B_{1g}), 235 cm^{-1} (combination of modes), 448 cm^{-1} (E_g) and 609 cm^{-1} (A_{1g}), in addition to some background in the ~ 75–750 cm^{-1} range] [22,26]. (The complete set of Raman spectra can be seen in SuppMater_Fig. S3.).

As expected, it is clear from the spectra of Fig. 2 the shift and broadening of the Raman lines at increasing temperatures [27]. Most importantly, these Raman results demonstrate that the observed temperature-induced modifications in the diffuse reflectance spectra of Fig. 1 are exclusively due to optical-electronic processes, and do not involve any structural transformation of the TiO_2 samples. In fact, the

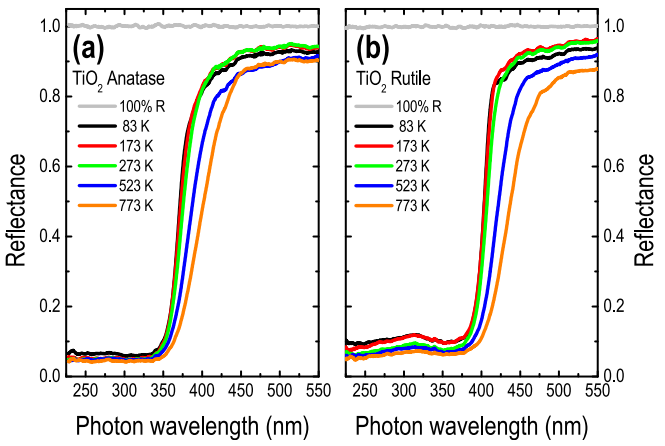

Fig. 1. Optical diffuse reflectance spectra, at some selected temperatures, of the (a) A-TiO_2 and (b) R-TiO_2 samples. The figures highlight the spectral region (225–550 nm range) where the optical absorption edges of TiO_2 typically occur. The 100 % reflectance curves (as obtained from a diffuse reflectance standard) are also shown.

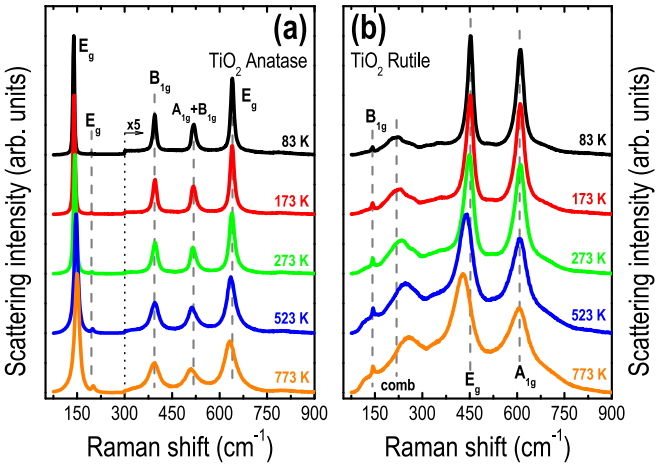

Fig. 2. Raman scattering spectra, at some selected temperatures, of the (a) A-TiO_2 and (b) R-TiO_2 samples. The figures show the most prominent phonon modes taking place in the Anatase and Rutile phases of TiO_2 (see text). In (a) the scattering intensities in the 300–900 cm^{-1} range were multiplied by 5. All spectra were normalized and vertically shifted for comparison reasons.

ensemble of experimental results suggests that the samples are (and remain) pure along the 83–823 K range [22], despite the diffuse reflectance and Raman spectra were acquired at increasing or decreasing temperatures and from different regions of the sample, therefore, confirming the appropriateness of the data.

Discussion

Among the various different features that a semiconductor material can exhibit its optical bandgap E_{gap} is of paramount importance. In combination with some theoretical work the E_{gap} (value and optical-related processes) can help to unravel the electronic structure of most materials, and knowing E_{gap} is essential to decide the purpose and operating range of semiconductor devices - specially the photon-based ones [28,29]. Investigating the temperature-dependent $E_{gap}(T)$ behavior provides additional information regarding the photon-electron–phonon interaction that, again, can improve the understanding and eventual application of several semiconductors. In practice, the E_{gap} values of nearly all materials can be obtained by means of optical measurements that take into account the energy range of interest as well

as details of the materials. The specifics of these measurements also influence the proper way to transform the experimental data into optical absorption spectra that, ultimately, will provide the corresponding E_{gap}.

In the case of powder-like samples, the optical diffuse reflectance spectra of Fig. 1 should be converted in a pseudo-absorption function F(R_∞) through the Schuster-Kubelka-Munk approximation: [30]

$$F(R_\infty) = \frac{(1-R_\infty)^2}{2R_\infty} \quad (1)$$

where R_∞ is the reflectance of the samples (as referred to a diffuse reflectance, non-absorbing standard). The results of this procedure can be seen in Fig. 3 that shows the F(R_∞) of the A-TiO_2 and R-TiO_2 samples at 83, 523 and 773 K, in the 2.5–4.0 eV photon energy range (or ~ 300–500 photon wavelength range).

At this point, the F(R_∞) spectra are further processed in order to determine the E_{gap}(T) of the TiO_2 samples. Considering that F(R_∞) corresponds to the optical absorption coefficient α [30], and given the indirect nature of the optical transitions of the A-TiO_2 sample its E_{gap} is obtained, traditionally [31], by extrapolating the linear least squares fit of $\alpha^{1/2}$ to zero, in a "$\alpha^{1/2}$ *versus* photon energy E" plot [32]. A similar reasoning applies to the direct bandgap of R-TiO_2 in which its E_{gap} derives from a "α^2 *versus* photon energy E" plot [33].

A more convenient way to obtain the E_{gap} values involves the fitting of the F(R_∞) (~absorption coefficient α) spectra with sigmoid-Boltzmann functions. The approach is straightforward (based on very efficient and reliable empirical relationships) and it is known to be exempt from errors due to experimental spectra acquisition and data processing [34]. Accordingly, the E_{gap}(T) of the present TiO_2 samples were achieved, after fitting the F(R_∞) spectra with sigmoid-Boltzmann functions (as shown in Fig. 3, for example), by considering:

$$E_{gap} = E_{Boltz}^{type} = E_0 - n_{type} \times \delta E \quad (2)$$

where E_0 and δE correspond, respectively, to the central energy and slope of the sigmoid-Boltzmann function [35], and n_{type} stands for the indirect or direct character of the optical transition (or bandgap), such that: $n_{IND} = 4.3$ and $n_{DIR} = 0.3$ [34].

Fig. 4 shows the Boltzmann-related E_0 energy and δE slope of the A-TiO_2 and R-TiO_2 samples in the whole 83–823 K temperature range. According to the figure, it is clear the variations experienced by E_0 and

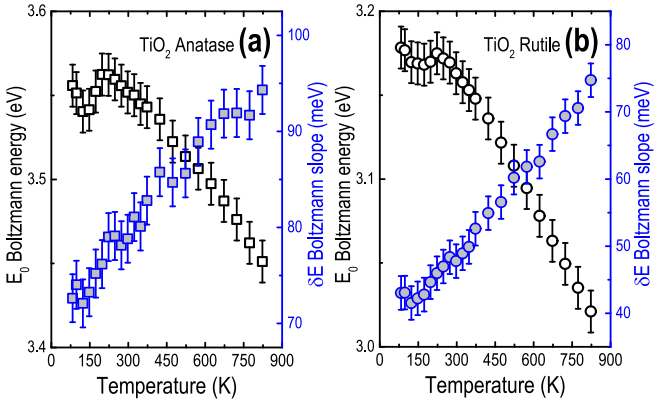

Fig. 4. Boltzmann-related energy E_0 and slope δE of the (a) A-TiO_2 and (b) R-TiO_2 samples, in the 83–823 K temperature range. The E_0 and δE values were obtained by fitting the experimental F(R_∞) spectra with sigmoid-Boltzmann functions, rendering error bars that denote the typical dispersion of the data. Notice the different energy ranges in (a) and (b).

δE as the temperature of measurement increases. In the first case E_0 downshifts and, in the latter, δE augments - both of them being associated with the (temperature-dependent) phonon-assisted processes taking place in the TiO_2 samples [31].

In combination with Eq.(2) - *i.e.*, $E_{Boltz}^{IND} = E_0 - 4.3 \times \delta E$ for A-TiO_2 and $E_{Boltz}^{DIR} = E_0 - 0.3 \times \delta E$ for R-TiO_2 - the data of Fig. 4 provide the E_{gap}(T) of the TiO_2 samples. These results are shown in Fig. 5, along with the E_{gap}(T) values available from the literature. As can be seen, the E_{gap}'s seem to be practically constant from 83 to ~ 300 K, with $E_{gap} = 3.24 \pm 0.03$ eV for A-TiO_2 and $E_{gap} = 3.16 \pm 0.03$ eV for R-TiO_2 and, then, the results indicate decreasing E_{gap} values as the temperature advances.

Regarding the data from literature, it is evident the overall decreasing E_{gap}(T) behavior presented by both phases as well as some deviation between the experimental E_{gap} values (except for those presented by Ref [24]). In this case the divergences may arise due to the use of films (with thicknesses below 100 nm) [23,25] or because of distinct measurement and/or E_{gap} evaluation methods. Being aware of these issues the present study considered TiO_2 samples with very well-established atom composition and structure, and sample-

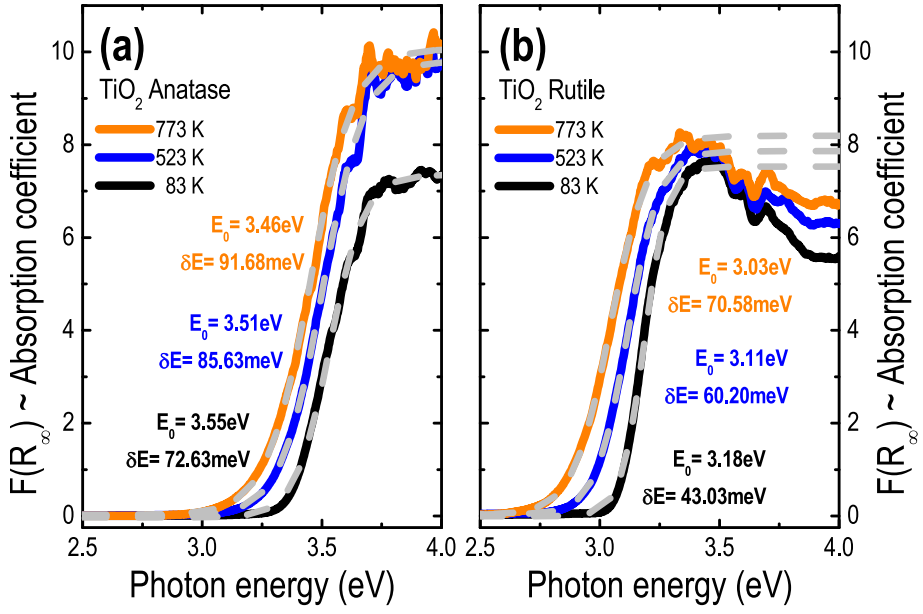

Fig. 3. Pseudo-absorption F(R_∞) spectra (solid lines), at some selected temperatures, of the (a) A-TiO_2 and (b) R-TiO_2 samples. The figures also display the corresponding sigmoid-Boltzmann fittings (dashed gray lines) and their corresponding E_0 (Boltzmann energy) and δE (Boltzmann slope) values.

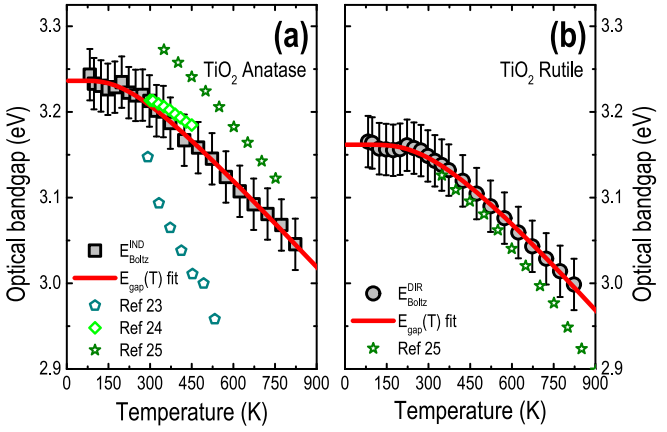

Fig. 5. Temperature-dependent optical bandgap $E_{gap}(T)$ of the (a) A-TiO_2 and (b) R-TiO_2 samples, as obtained from diffuse reflectance measurements. The figures also display the results from other works [23–25], as well as the fitting of the $E_{gap}(T)$ data with Eq.(3). The energy ranges in (a) and in (b) were kept the same for comparison reasons.

measurements conditions that guarantee thermal equilibrium and efficient light reflection–absorption - namely, the samples are thick enough, densely-packed, and constituted by randomly-shaped particles whose sizes are in the order of the wavelength of the incoming radiation [30,34]. Furthermore, for comparison reasons, the $E_{gap}(T)$ of the A-TiO_2 and R-TiO_2 samples were additionally obtained by means of the conventional methods (*i.e.*, linear extrapolation of the "$\alpha^{1/2}$ or α^2 *versus* photon energy E" plots). As a result, within the experimental error (E_{gap} ± 30 meV), no appreciable differences were observed in the present E_{gap} values - neither involving the use of different methods to estimate E_{gap} nor by adopting dwell times of 5 min or 30 min. (The $E_{gap}(T)$ results by applying different evaluation methods, along with those relating different dwell times, can be seen in SuppMater_Fig. S4.)

Still relating to the results of Fig. 5, so far, different approaches have been considered to investigate the shift of the energy levels in semiconductor materials and, therefore, to explain their temperature-dependent E_{gap} behavior. Among them, one can mention the pioneering work involving the contraction–expansion of semiconductor crystal lattices and their respective electron–phonon interaction [36,37] that, allied to meticulous experimental results [38], advanced the understanding of $E_{gap}(T)$. Given its practical importance the $E_{gap}(T)$ behavior has been described in terms of (semi-)empirical models as well. As a result, some of the existing $E_{gap}(T)$ approaches are very popular (in spite of serious conceptual flaws) [39], others depend on (not always readily available or reliable) specific quantities [40], whereas a few ones (based on simple-reasonable groundings) [41] provide exceptional agreement with the experimental data - Refs [42,43] present good reviews on the subject. Within this context it is believed that the access to consistent $E_{gap}(T)$ databases (ideally involving different materials and extended measurements conditions) can contribute to unravel the mechanisms behind the temperature-dependent photon-electron–phonon interactions. For that reason, the current $E_{gap}(T)$ data of the A-TiO_2 and R-TiO_2 samples were analyzed by considering the three-parameter (thermodynamic) function:[37,41]

$$E_{gap}(T) = E_{gap}(0) - S\langle\hbar\omega\rangle\left[\coth\left(\frac{\langle\hbar\omega\rangle}{2k_BT}\right) - 1\right] \quad (3)$$

where $E_{gap}(0)$ is the optical bandgap value at T = 0 K, S is a dimensionless coupling constant, $\langle\hbar\omega\rangle$ is the average phonon energy, and k_B stands for the Boltzmann constant.

As can be seen from Fig. 5, Eq.(3) perfectly fits the experimental $E_{gap}(T)$ data in the 83–823 K temperature range by providing $E_{gap}(0)$'s equal to 3.23(6) and 3.16(2) eV for A-TiO_2 and R-TiO_2, respectively. Regarding the average phonon frequency, for both polymorphs, $\langle\hbar\omega\rangle$ stays around 50–80 meV which is in the same range (approx. 450–650 cm^{-1}) of the Raman results (Fig. 2), and close to the Boltzmann-related δE slopes (Fig. 4). Obviously, this association is not fortuitous and more investigations (including other semiconductor materials and distinct optical characterization techniques) are under way to make it clear.

For comparison purposes the $E_{gap}(T)$ data of Fig. 5 were also analyzed according to the standard (Varshni's) expression $E_{gap}(T) = E_{gap}(0) - \frac{\alpha T^2}{\beta+T}$ where α and β are fitting parameters (such that, as it was originally proposed [39], β ~ Debye temperature). Even though the Varshni's expression reproduced the experimental $E_{gap}(T)$ with good precision and retrieved $E_{gap}(0)$ values similar to those achieved with Eq. (3), the obtained β parameters are far from the supposed TiO_2-related Debye temperatures θ_D. More precisely, whereas the literature indicates θ_D's in the 500–600 K range, for both phases of TiO_2 [2], the fitting procedure yields β(A-TiO_2) = 800 K and β(R-TiO_2) = 4150 K (see SuppMat_Fig. S5).

In view of that, according to the present experimental results, the temperature-dependent optical bandgap of the A-TiO_2 and R-TiO_2 samples can be properly described by:

$$E_{gap}^{A-TiO_2}(T) = 3.24 - 0.12\left[\coth\left(\frac{0.057}{2k_BT}\right) - 1\right] \quad (4)$$

and

$$E_{gap}^{R-TiO_2}(T) = 3.16 - 0.18\left[\coth\left(\frac{0.083}{2k_BT}\right) - 1\right] \quad (5)$$

The current work could be complemented by extending the range of temperatures and/or by measuring TiO_2 in the form of bulk (wafer) samples or thick films, allowing to explore the effects due to the Anatase-to-Rutile phase transformation as well as those originating from disorder, for example. Anyway, in its present form, this work investigated TiO_2 powder-like samples of very well-known composition and structure, considered optical reflectance and Raman scattering measurements (over a considerable temperature range), and performed a rather critical data analysis-discussion. As a result, it was possible to obtain (for the first time) reliable E_{gap} values and to establish accurate mathematical expressions that describe the temperature-dependent E_{gap} behavior of the Anatase and Rutile phases of TiO_2.

Concluding remarks

The Anatase and Rutile polymorphs of titanium dioxide TiO_2 occupy a very privileged position in the area of photon-related or solar-driven applications such as those involving, for instance: pigments, optical coatings, energy production-storage processes, etc. Much of this success derives from the singular properties of TiO_2 as well as from its systematic investigation along the years. Yet, the temperature-dependent optical bandgap $E_{gap}(T)$ behavior of A-TiO_2 and R-TiO_2 was still incomplete or has not been explored adequately. In view of that, this work shows a detailed $E_{gap}(T)$ investigation, in the 83–823 range, by considering powder-like A-TiO_2 and R-TiO_2 samples of recognized chemical composition and atomic structure. The experimental data were analyzed thoroughly (by exploring different methods to evaluate E_{gap} and the $E_{gap}(T)$ results) rendering the following expressions $E_{gap}^{A-TiO_2}(T) = 3.24 - 0.12\left[\coth\left(\frac{0.057}{2k_BT}\right) - 1\right]$ and $E_{gap}^{R-TiO_2}(T) = 3.16 - 0.18\left[\coth\left(\frac{0.083}{2k_BT}\right) - 1\right]$ that precisely describe the temperature-dependent E_{gap} behavior of A-TiO_2 and R-TiO_2. Taking into consideration all of these aspects, the present work is expected to contribute with the study of new materials and/or devices based, total or partially, onto the Anatase or Rutile phases of TiO_2.

CRediT authorship contribution statement

A.R. Zanatta: Writing – review & editing, Writing – original draft,

Validation, Resources, Methodology, Investigation, Funding acquisition, Formal analysis, Data curation, Conceptualization.

Declaration of competing interest

The authors declare that they have no known competing financial interests or personal relationships that could have appeared to influence the work reported in this paper.

Data availability

Data will be made available on request.

Acknowledgments

This work was financially supported by the Brazilian agencies CNPq (Grant 304569/2021-6) and FAPESP.

Appendix A. Supplementary data

Supplementary data to this article can be found online at https://doi.org/10.1016/j.rinp.2024.107653.

References

[1] See, for example, F. Parrino and L. Palmisano, Introduction, in *Titanium dioxide (TiO_2) and its applications*, Edited by F. Parrino and L. Palmisano (Elsevier 2021). Chap. 1. https://doi.org/10.1016/B978-0-12-819960-2.00018-3.
[2] Howard CJ, Sabine TM, Dickson F. Structural and thermal parameters for Rutile and Anatase. Acta Cryst 1991;B47:462. https://doi.org/10.1107/S010876819100335X.
[3] D. R.Coronado, G. R. Gattorno, M. E. E. Pesqueira, C. Cab, R. Coss, and G. Oskam, Phase-pure TiO_2 nanoparticles: Anatase, Brookite and Rutile. Nanotechnology 19 (2008) 145605. http://doi.org/ 10.1088/0957-4484/19/14/145605.
[4] Zhu T, Gao SP. The stability, electronic structure, and optical property of TiO_2 polymorphs. J Phys Chem C 2014;118:11385. https://doi.org/10.1021/jp412462m.
[5] Zanatta AR, Cemin F, Echeverrigaray FG, Alvarez F. On the relationship between the Raman scattering features and the Ti-related chemical states of $Ti_xO_yN_z$ films. J Mater Res Technol 2021;14:864. https://doi.org/10.1016/j.jmrt.2021.06.090.
[6] Echeverrigaray FG, Zanatta AR, Alvarez F. Reducible oxide and allotropic transition induced by hydrogen annealing: synthesis routes of TiO_2 thin films to tailor optical response. J Mater Res Technol 2021;12:1623. https://doi.org/10.1016/j.jmrt.2021.03.082.
[7] Zanatta AR. Assessing the amount of the Anatase and Rutile phases of TiO_2 by optical reflectance measurements. Res Phys 2021;22:103864. https://doi.org/10.1016/j.rinp.2021.103864.
[8] Zanatta AR, Echeverrigaray FG, Cemin F, Alvarez F. Gradual and selective achievement of Rutile-TiO_2 by thermal annealing amorphous $Ti_xO_yN_z$ films. J Non-Crystal Solids 2022;579:121375. https://doi.org/10.1016/j.jnoncrysol.2021.121375.
[9] Hanaor DAH, Sorrell CC. Review of the Anatase to Rutile phase transformation. J Mater Sci 2011;46:855. https://doi.org/10.1007/s10853-010-5113-0.
[10] Fujishima A, Honda K. Electrochemical photolysis of water at a semiconductor electrode. Nature 1972;238:37. https://doi.org/10.1038/238037a0.
[11] Fujishima A, Zhang X, Tryk DA. TiO_2 photocatalysis and related surface phenomena. Surf Sci Rep 2008;63:515. https://doi.org/10.1016/j.surfrep.2008.10.001.
[12] J. Nowotny, Applications, in *Oxide semiconductors for Solar energy conversion: Titanium dioxide* (CRC Press, Boca Raton, 2012), Chap 8. ISBN 978-1-4398-4839-5.
[13] Bai Y, Seró IM, Angelis F, Bisquert J, Wang P. Titanium dioxide nanomaterials for photovoltaic applications. Chem Rev 2014;114:10095. https://doi.org/10.1021/cr400606n.
[14] Bai J, Zhou B. Titanium dioxide nanomaterials for sensor applications. Chem Rev 2014;114:10131. https://doi.org/10.1021/cr400625j.
[15] T. Parangi and M. K. Mishra, Titanium dioxide as energy storage material: A review on recent advancement, in *Titanium Dioxide - Advances and Applications*, Edited by H. M. Ali (IntechOpen, 2022). Chap 2.
[16] Rajh T, Dimitrijevic NM, Bissonnette M, Koritarov T, Konda V. Titanium dioxide in the service of the biomedical revolution. Chem Rev 2014;114:10177. https://doi.org/10.1021/cr500029g.
[17] Titanium dioxide (TiO_2) market size, share & trends analysis report by application (Paints & Coatings, Plastics, Pulp & Paper, Cosmetics), Report ID: 978-1-68038-705-6 (2019). https://www.grandviewresearch.com/industry-analysis/titaniumdioxide-industry.
[18] Lee CP, Lin LY, Tsai KW, Vittal R, Ho KC. Enhanced performance of dye-sensitized solar cell with thermally-treated TiN in its TiO_2 film prepared at low temperature. J Power Sources 2011;196:1632. https://doi.org/10.1016/j.jpowsour.2010.09.022.
[19] Yella A, Heiniger LP, Gao P, Nazeeruddin MK, Gratzel M. Nanocrystalline Rutile electron extraction layer enables low-temperature solution processed perovskite photovoltaics with 13.7% efficiency. Nano Lett 2014;14:2591. https://doi.org/10.1021/nl500399m.
[20] Yun TK, Park SS, Kim D, Shim JH, Bae JY, Huh S, et al. Effect of the Rutile content on the photovoltaic performance of the dye-sensitized solar cells composed of mixed-phase TiO_2 photoelectrodes. Dalton Trans 2012;41:1284. https://doi.org/10.1039/C1DT11765C.
[21] Spurr RA, Myers H. Quantitative analysis of Anatase-Rutile mixtures with an x-ray diffractometer. Anal Chem 1957;29:760. https://doi.org/10.1021/ac60125a006.
[22] Zanatta AR. A fast-reliable methodology to estimate the concentration of Rutile or Anatase phases of TiO_2. AIP Adv 2017;7:075201. https://doi.org/10.1063/1.4992130.
[23] Zhang F, Zhang RJ, Zhang DX, Wang ZY, Xu JP, Zheng YX, et al. Temperature-dependent optical properties of titanium oxide thin films studied by spectroscopic ellipsometry. App Phys Exp 2013;6:121101. https://doi.org/10.7567/APEX.6.121101.
[24] Mishra V, Warshi MK, Sati A, Kumar A, Mishra V, Kumar R, et al. Investigation of temperature-dependent optical properties of TiO_2 using diffuse reflectance spectroscopy. SN Appl Sci 2019;1:241. https://doi.org/10.1007/s42452-019-0253-6.
[25] Wu YN, Wuenschell JK, Fryer R, Saidi WA, Ohodnicki P, Chorpening B, et al. Theoretical and experimental study of temperature effect on electronic and optical properties of TiO_2: comparing Rutile and Anatase. J Phys: Condens Matter 2020;32:405705. https://doi.org/10.1088/1361-648X/ab9d4f.
[26] Porto SPS, Fleury PA, Damen TC. Raman spectra of TiO_2, MgF_2, ZnF_2, FeF_2, and MnF_2. Phys Rev 1967;154:522. https://doi.org/10.1103/physrev.154.522.
[27] See, for example, A. R. Zanatta, Temperature-dependent Raman scattering of the Ge+GeO_x system and its potential as an optical thermometer. Res Phys 19 (2020) 103500. https://doi.org/10.1016/j.rinp.2020.103500.
[28] S. M. Sze, Photonic devices, in *Semiconductor devices: Physics and technology* (John Wiley & Sons, Singapore, 1985). Chap 7. TK7871.85.S9883 1985.
[29] P. Bhattacharya, Optical processes in semiconductors, in *Semiconductor optoelectronic devices* (Prentice Hall, New York, 1994). Chap 3. ISBN 0-13-489766-8.
[30] H. G. Hecht, The present status of diffuse reflectance theory, in *Modern Aspects of reflectance spectroscopy*. Edited by W. W. Wendlandt (Springer, Boston, 1968). Chap 1. https://doi.org/10.1007/978-1-4684-7182-3_1.
[31] See, for example, M. Fox, Interband absorption, in *Optical properties of solids* (Oxford Univ. Press, Oxford, 2008). Chap 3. ISBN 978-0-19-850613-3.
[32] MacFarlane GG, Roberts V. Infrared absorption of silicon near the lattice edge. Phys Rev 1955;98:1865. https://doi.org/10.1103/PhysRev.98.1865.
[33] MacFarlane GG, Roberts V. Infrared absorption of germanium near the lattice edge. Phys Rev 1955;97:1714. https://doi.org/10.1103/PhysRev.97.1714.2.
[34] Zanatta AR. Revisiting the optical bandgap of semiconductors and the proposal of a unified methodology to its determination. Sci Rep 2019;9:11225. https://doi.org/10.1038/s41598-019-47670-y.
[35] F. E. Harrell Jr., Binary logistic regression, in *Regression modeling strategies: With applications to linear models, logistic regression, and survival analysis* (Springer-Verlag, New York, 2001). Chap 10. ISBN 0-387-95232-2.
[36] W. Shockley and J. Bardeen, Energy bands and mobilities in monatomic semiconductors. Phys Rev 77 (1950) 407. https://doi.org/10.1103/PhysRev.77.407 & J. Bardeen and W. Shockley, Deformation potentials and mobilities in non-polar crystals. Phys Rev 80 (1950) 72. https://doi.org/10.1103/PhysRev.80.72.
[37] H. Y. Fan, Temperature dependence of the energy gap in monatomic semiconductors. Phys Rev 78 (1950) 808. https://doi.org/10.1103/PhysRev.78.808.2 & H. Y. Fan, Temperature dependence of the energy gap in semiconductors. Phys Rev 82 (1951) 900. https://doi.org/10.1103/PhysRev.82.900.
[38] G. G. MacFarlane, T. P. McLean, J. E. Quarrington, and V. Roberts, Fine structure in the absorption-edge spectrum of Ge. Phys Rev 108 (1957) 1377. https://doi.org/10.1103/PhysRev.108.1377 & G. G. MacFarlane, T. P. McLean, J. E. Quarrington, and V. Roberts, Fine structure in the absorption-edge spectrum of Si. Phys Rev 111 (1958) 1245. https://doi.org/10.1103/PhysRev.111.1245.
[39] Varshni YP. Temperature dependence of the energy gap in semiconductors. Physica 1967;34:149. https://doi.org/10.1016/0031-8914(67)90062-6.
[40] A. Manoogian and A. Leclerc, Determination of the dilation and vibrational contributions to the energy band gaps in germanium and silicon. phys stat sol (b) 92 (1979) K23.
[41] O'Donnell KP, Chen X. Temperature dependence of semiconductor band gaps. Appl Phys Lett 1991;58:2924. https://doi.org/10.1063/1.104723.
[42] R. Pässler, Semi-empirical descriptions of temperature dependences of band gaps in semiconductors. phys stat sol (b) 236 (2003) 710. https://doi.org/10.1002/pssb.200301752.
[43] Cardona M, Kremer RK. Temperature dependence of the electronic gaps of semiconductors. Thin Solid Films 2014;571:680. https://doi.org/10.1016/j.tsf.2013.10.157.